JOC*Note*

Biocatalytic Microcontact Printing

Phillip W. Snyder,[†] Matthew S. Johannes,[‡] Briana N. Vogen,[†] Robert L. Clark,*[,‡] and Eric J. Toone*[,†]

Department of Chemistry, Duke University, Durham, North Carolina, 27708-0346, and The Pratt School of Engineering, Duke University, Durham, North Carolina, 27708-0271

rclark@egr.duke.edu; eric.toone@duke.edu

Received June 7, 2007

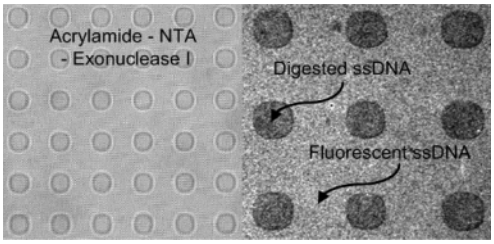

Immobilized biocatalytic lithography is presented as an application of soft lithography. In traditional microcontact printing, diffusion limits resolution of pattern transfer. By using an immobilized catalyst, the lateral resolution of microcontact printing would depend only on the length and flexibility of the tether (<2 nm) as opposed to diffusion (>100 nm). In the work, exonuclease reversibly immobilized on a relief-patterned stamp is used to ablate ssDNA monolayers Percent of ablation was determined via confocal fluorescence microscopy to be ~70%.

Microcontact printing (μCP) has gained broad acceptance for the rapid high-resolution transfer of patterns over large surface areas.[1] The resolution limits of μCP are determined at least in part by ink diffusion. Efficient transfer of low molecular weight (<200 Da) inks from PDMS stamps requires stamp−substrate contact times of 10−1000 s.[2] During this period, both lateral diffusion of ink across the substrate and gas-phase transfer from the stamp blur feature edges, and the practical limit to horizontal dimensions for defect-free patterns is in excess of 100 nm.[3]

Pattern transfer achieved by a nondiffusive process would potentially improve the lateral resolution of μCP to the sub-100 nm domain. Nondiffusive pattern transfer might be achieved with an immobilized catalyst, through modification of a cognate reactivity on an apposing face. In 2003, Reinhoudt and co-workers patterned a gold surface functionalized with silyl ethers using a stamp bearing acidic moieties, in turn incorporated onto the stamp by plasma etching.[4] Although pattern transfer was clear, the process effected cleavage of only 30% of the reactive moieties during 30 min of contact: the low level of pattern transfer presumably occurs due either to low concentrations of acid moieties or from inhomogeneities across the surface of the stamp. Protons are also promiscuous catalysts, promoting myriad transformations, and free to diffuse laterally across the stamp surface, limiting the broader utility of the method.

As a class of catalysts, enzymes offer both diverse chemistry and exquisite specificity. Several groups have exploited this specificity in dip-pen nanolithography.[5] In these approaches, enzyme is either covalently bound or physisorbed on an AFM tip and used to "write" by controlled translocation of the tip across a substrate-bearing surface. Such processes are serial and not amenable to high-throughput applications. Here, we present a proof-of-concept demonstration of catalytic parallel lithography, using stamp-immobilized enzyme to transfer pattern to a cognate substrate. Because the catalyst is immobilized on the stamp surface, the diffusion limitation of traditional μCP is obviated and the lateral resolution is controlled only by the length and flexibility of the catalyst tether.

Our process requires a stamp with properties supportive of both dense immobilization of catalyst and the requirements of soft lithography. Poly(acrylamide) stamps offer a number of advantages consistent with both requirements. Poly(acrylamide) is elastomeric, assuring conformal contact between stamp and substrate as well as biocompatible and wettable, providing a suitable surface for enzymatic activity.[6,7] Finally, synthetic elaboration of acrylate monomers facilitates specific immobilization of enzyme catalyst.

Noncovalent enzyme immobilization provides reversible stamp "inking", and we used a nitrilotriacetic acid·nickel(II) complex to immobilize hexahistidine-tagged enzyme onto a hydrogel stamp. This system facilitates both replacement of inactive or degraded enzyme with new catalyst and the adhesion of an alternative catalyst with different chemical reactivity: immobilization is reversed by the addition of nickel chelators such as EDTA or imidazole. The construction of nickel-chelating poly(acrylamide) hydrogels required an acrylate monomer bearing nitrilotriacetic acid (**1**, Figure 1), readily prepared from lysine.[8]

With a polymerizable NTA derivative in hand, we turned to stamp fabrication protocols. An aqueous solution of NTA-acrylamide **1** and commercial acrylamide/bisacrylamide was

[†] Department of Chemistry.
[‡] The Pratt School of Engineering.

(1) (a) Quist, A. P.; Pavlovic, E.; Oscarsson, S. *Anal. Bioanal. Chem.* **2005**, *381*, 591−600. (b) Li, X. M.; Huskens, J.; Reinhoudt, D. N. *J. Mater. Chem.* **2004**, *14*, 2954−2971.

(2) Libioulle, L.; Bietsch, A.; Schmid, H.; Michel, B.; Delamarche, E. *Langmuir* **1999**, *15*, 300−304.

(3) (a) Delamarche, E.; Schmid, H.; Bietsch, A.; Larsen, N. B.; Rothuizen, H.; Michel, B.; Biebuyck, H. *J. Phys. Chem. B* **1998**, *102*, 3324- 3334. (b) Michel, B.; Bernard, A.; Bietsch, A.; Delamarche, E.; Geissler, M.; Juncker, D.; Kind, H.; Renault, J. P.; Rothuizen, H.; Schmid, H.; Schmidt-Winkel, P.; Stutz, R.; Wolf, H. *IBM J. Res. Dev.* **2001**, *45*, 697−719.

(4) Li, X. M.; Peter, M.; Huskens, J.; Reinhoudt, D. N. *Nano Lett.* **2003**, *3*, 1449−1453.

(5) (a) Takeda, S.; Nakamura, C.; Miyamoto, C.; Nakamura, N.; Kageshima, M.; Tokumoto, H.; Miyake, J. *Nano Lett.* **2003**, *3*, 1471−1474. (b) Xu, P.; Uyama, H.; Whitten, J. E.; Kobayashi, S.; Kaplan, D. L. *J. Am. Chem. Soc.* **2005**, *127*, 11745−11753. (c) Hyun, J.; Kim, J.; Craig, S. L.; Chilkoti, A. *J. Am. Chem. Soc.* **2004**, *126*, 4770−4771. (d) Riemenschneider, L.; Blank, S.; Radmacher, M. *Nano Lett.* **2005**, *5*, 1643−1646.

(6) Popovic, S.; Tamagawa, H.; Taya, M. *Proc. SPIE Smart Struct. Mater.* **2000**, *3987*, 177−186.

(7) (a) Schlaff, S. *Endocrinology* **1976**, *98*, 527−533. (b) Gotoh, Y.; Nishida, E.; Yamashita, T.; Hoshi, M.; Kawakami, M.; Sakai, H. *Eur. J. Biochem.* **1990**, *193*, 661−669. (c) Matsuda, S.; Kawasaki, H.; Moriguchi, T.; Gotoh, Y.; Nishida, E. *J. Biol. Chem.* **1995**, *270*, 12781−12786.

(8) Hochuli, E.; Dobeli, H.; Schacher, A. *J. Chromatogr. A* **1987**, *411*, 177−184.

10.1021/jo0711541 CCC: $37.00
Published on Web 08/18/2007

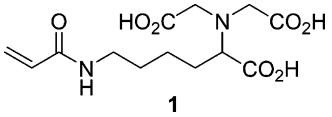

1

FIGURE 1. Acrylamidonitrilotriacetic acid monomer.[8]

allowed to polymerize in the presence of ammonium persulfate and tetramethylethylenediamine under a suspended silicon−PMMA master. Following polymerization, the stamp was removed from the master, cut to 1 cm^2 squares, and placed in 50 mM $NiSO_4$. After incubation with Ni^{2+}, the stamps took on a green hue, indicating the presence of chelated nickel.

To test the ability of immobilized enzyme to execute chemistry at a surface, we utilized the enzyme−substrate system of exonuclease I (exoI) and single-stranded DNA (ssDNA); this system offers several advantages. ExoI has no cofactor requirements, and a construct bearing a *C*-terminal His_6-tag has been cloned into a pET vector.[9] Additionally, synthetic oligonucleotides are commercially available with modifications that facilitate immobilization and imaging; various immobilization strategies for ssDNA have been described.[10] The sequence 5′-GATTACAGATTACA-3′ bearing 5′-aminohexyl and 3′-cyTAMRA modifications was used to immobilize substrate on isothiocyanate-modified glass substrates; the identical sequence bearing 5′-mercaptohexyl modification was used to immobilize substrate on gold surfaces.

ExoI was deposited on immobilized nickel stamps during immersion in a solution of enzyme (0.1 μM) for 10 min. The stamp was sonicated three times in a 0.1% sodium dodecylsulfate (SDS) solution for 5 min to remove nonspecifically adsorbed enzyme. Glass slides bearing ssDNA labeled with TAMRA dye were placed atop stamps bearing immobilized enzyme which, in turn, rested on filter paper soaked in magnesium reaction buffer. Reaction times were varied from 1 to 12 h at 4 °C.

Following incubation, glass slides were imaged by confocal fluorescence microscopy. Figure 2a illustrates the transfer of pattern features from stamp to substrate through the catalytic activity of exoI on ssDNA. Contact between the stamp and surface leads to the ablation of DNA and release of the fluorescent dye, and pattern transfer is indicated by the appearance of dark regions. Pattern transfer is consistent across the exposed surface area (Figure 2c). The extent of ablation was determined by comparison of fluorescent intensity difference inside and outside exposed area and corresponds to 69.2 ± 16.9% removal of fluorophore. The identical experiment conducted with flat stamps showed 63.8 ± 15.5% removal of fluorophor (see the Supporting Information).

Patterned DNA hydrolysis on gold was observed by AFM imaging in contact mode (Figure 2b). Figure 2c shows a friction AFM cross-sectional image of a self-assembled monolayer patterned using biocatalytic-μCP. Although low in sensitivity by comparison to fluorescence microscopy, the AFM data demonstrate both the feature resolution near the pattern edge

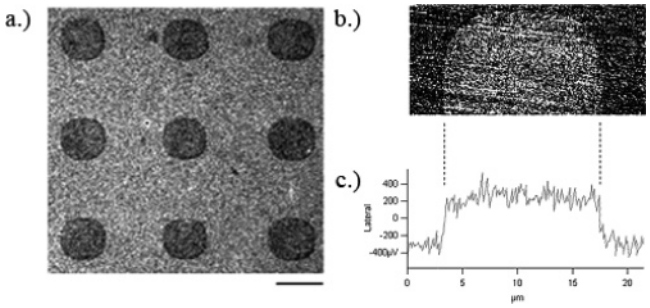

FIGURE 2. (a) Confocal microscopy image of fluorescently labeled ssDNA patterned by enzymatic microcontact printing. Glass slides functionalized with isothiocyanate were incubated with 5′-hexylaminated, 3′-fluorescently labeled DNA and printed with an NTA-stamp bearing exonuclease I. Stamp dimensions are exactly reproduced on the DNA monolayer. 100× magnification; 10 μm scalebar. (b) AFM friction image of a single feature created by enzymatic digestion of ssDNA. Length scale is indicated below. (c) Line profile of the above AFM image. The imaged features were created using a stamp with different sized protrusions than that used in Figure 2a, but in the same experimental run.

and the uniformity of pattern across the feature. Statistical analysis of the noise inside and outside the pattern shows essentially identical levels: over 20 000 points the root mean square (rms) deviation inside the pattern is 85 μV, while the surface area outside the pattern produced an rms deviation of 89 μV. The signal-to-noise ratio is roughly 10-fold (630 to 87 μV), and the difference in the noise mean for the two regions (4 μV) is 20-fold less than the mean of the noise (87 μV). Together, these observations suggest that surface "roughness" is equivalent inside and outside the ablated pattern.

The results presented here demonstrate the feasibility of transferring a relief pattern from a stamp bearing an immobilized highly specific biocatalyst to a surface coated with complementary functionality via chemical reaction. The process is not limited to ablative spatial differentiation: surface chemistry could be patterned by additive or redox transformation as well. The technique offers the potential to synthesize surface structures through serial stamping steps with different catalysts in each step. Although the application of biological catalysts offers an enormous variety of chemistries interchanged by virtue of reversible immobilization strategies, the method is by no means limited to the use of enzymes. In combination with reversible catalyst switching, these modulations of surface chemistries could be used in combinatorial fashion to manufacture materials with unique complexity.

In conclusion, we have demonstrated the feasibility of biocatalytic lithography. The key aspects of this methodology are as follows: (1) the reversible immobilization of enzyme on (2) a relief patterned poly(acrylamide) stamp bearing the nickel chelate nitrilotriacetic acid to (3) ablate substrate presented on an opposing surface in a pattern-dependent fashion. Catalyst-mediated soft lithographic technique offers the advantage of lateral resolution controlled by the range of motion of the immobilized catalyst rather than by the diffusive properties of molecular inks. This feature should facilitate the implementation of strategies for stamping nanoscale features. Further examination of stamping parameters and the application of this methodology to nanolithography are underway, and we will report our results in due course.

(9) (a) Lehman, I. R.; Nussbaum, A. L. *J. Biol. Chem.* **1964**, *239*, 2628−2636. (b) Breyer, W. A.; Matthews, B. W. *Nat. Struct. Biol.* **2000**, *7*, 1125−1128.

(10) (a) Herne, T. M.; Tarlov, M. J. *J. Am. Chem. Soc.* **1997**, *119*, 8916−8920. (b) Guo, Z.; Guilfoyle, R. A.; Thiel, A. J.; Wang, R.; Smith, L. M. *Nucl. Acids Res.* **1994**, *22*, 5456−5465.

(11) Gao, C.; Lin, C.-H.; Lo, C.-H. L.; Mao, S.; Wirsching, P.; Lerner, R. A.; Janda, K. D. *Proc. Natl. Acad. Sci. U.S.A.* **1997**, *94*, 11777−11782.

Experimental Section

General Procedure for Biocatalytic Microcontact Printing. All solutions were filtered through a 0.22 μm filter and stored in closed containers except during use. Silicon−PMMA masters were stored covered and cleaned with water and dried under a stream of N_2 immediately subsequent to stamp manufacture. Fresh stamps were made prior to each experiment. Exonuclease I activity could be assayed in solution by mixing a 1 μM solution of enzyme with 10 μM solution of oligonucleotide and incubating for 1 h. The resulting solution was lyophilized and submitted for MALDI-MS. Active enzyme completely obliterated the mass peak for oligonucleotide relative to a control sample lacking enzyme.

The gene for wild type exonuclease I was obtained by PCR amplification from the genome of *E. coli* DH5, digested with *NdeI* and *XhoI*, and ligated into a similarly prepared pET22b overexpression vector (a generous gift from Dr. B. W. Matthews, University of Oregon). The resulting construct was transformed into BL21 DE3 cells via heat shock. ExoI was expressed and purified following standard IMAC protocols. Single colonies from this transformation were grown to an $OD_{600} = 0.6-0.8$, induced for 4 h at 37 °C with 125 mg L^{-1} isopropyl thiogalactopyranoside and harvested by centrifugation. The construct yielded roughly 5 mg protein per liter of cell growth. Protein was purified in a standard fashion over nickel affinity resin using one half the standard imidazole concentration for the wash buffer (30 mM imidazole).

N^{ϵ}-Acrylamido-N^{α}-bis(carboxymethyl)lysine (**3**) (25 mg) was dissolved in a solution of 300 μL of commercially available 40% acrylamide/ bis-acrylamide (19:1) and 200 μL of 1.5 M tris, pH = 8.8. To this prepolymer were added 10 μL of 20% (w/v) aqueous ammonium persulfate and 0.4 μL of tetramethylethylenediamine. After brief but vigorous agitation, 185 μL of this solution was quickly aliquoted onto a polyethylene plate between two 1.5 mm spacers and the silicon-PMMA master, adhered to a separate polyethylene plate, was suspended in contact with the solution while resting on the spacers. Following polymerization (typically 5−15 min), the stamp was carefully removed from the master and submerged in aqueous 50 mM $NiSO_4$ in a small Petri dish.

All solutions were cooled to ∼4 °C prior to use. The nickel-chelating stamp was rinsed with 2 mL of binding buffer (0.5 mM imidazole, 20 mM NaCl, 5 mM Tris, pH = 7.90) and immersed in a solution of His-tagged exoI (0.1 μM) in binding buffer for 1 min. The stamp was rinsed in binding buffer and wash buffer (60 mM imidazole, 20 mM NaCl, and 5 mM Tris, pH = 7.90) and then removed to a 50 mL conical vial containing 0.05% SDS and sonicated for 2 min. The stamp was removed to a fresh Petri and washed with binding buffer, wash buffer, and reaction buffer (66 mM glycine, 12 mM $MgCl_2$, pH = 9.50). The processed stamp was then placed in a large Petri dish on a Whatman filter paper soaked with reaction buffer and allowed to equilibrate for 5 min.

Gold or glass substrates were placed atop stamps, and gentle pressure was applied to achieve contact. Attainment of proper pressure was complicated in the case of gold substrates as these substrates were opaque and existing air bubbles between stamp and substrate could not be visualized. On the other hand, the transparent glass slides facilitated the stamping procedure as pressure was applied until conformal contact was achieved. Stamps with adhered substrates were sealed in Petri dishes with Parafilm and maintained at 4 °C for 1−14 h. Following incubation, substrates were removed and immediately immersed in room-temperature 50 mM EDTA (volumetric standard), rinsed with ddH_2O, and dried under a stream of N_2.

DNA Immobilization on Gold Substrates. All oligonucleotides were purchased from Integrated DNA Technologies (IDT) with 5′-mercaptohexyl modification of the sequence 5′-GATTACAGATTACA-3′ for immobilization on gold substrates. Gold substrates (∼ 1 cm × 1 cm) were manufactured by coating silicon chips with a 70 Å chromium adhesion layer followed by 230 Å gold layer using an electron-beam metal evaporator (CHA Industries). Thiolated oligonucleotides were purified by passage over Sepharose following standard procedures provided by IDT. Substrates were immersed in a 1 μM solution of purified thiolated oligonucleotide in 800 mM K_2PO_4, pH = 5.0 for 2 h, rinsed with this buffer, and immersed in a solution of 1 mM mercaptohexanol in water for 1 h. Finally, substrates were removed, rinsed in water, and incubated in reaction buffer (vide supra) until needed. Generally, gold substrates were used within 24 h of preparation.

DNA Immobilization on Glass Substrates. All oligonucleotides were purchased from Integrated DNA Technologies (IDT) with 5′-aminohexyl, 3′-cyTAMRA modification of the sequence 5′-GATTACAGATTACA-3′ for immobilization on isothiocyanate functionalized slides. The oligonucleotides were dissolved in ddH_2O with a final concentration of 100 μM and stored at −20 °C in a opaque tube as such. Prior to immobilization, oligonucleotides were diluted in sterile filtered PBS pH = 7.00 to a final DNA concentration between 0.1 and 10 μM. Three aliquots (100 μL) of the oligonucleotide solutions were placed atop isothiocyanate slides (Genorama) and allowed to incubate for 2 to 24 h at room temperature. Following DNA deposition, the solutions were removed by aspiration and rinsed carefully while aspirating. Slides were then incubated with reaction buffer (vide supra) until used. Although not measured, water contact angles were qualitatively different between regions of the slide functionalized and unfunctionalized with oligonucleotide. Specifically, unfunctionalized regions were resistant to wetting with water. Mild to moderate color/ intensity changes were evident with variations in incubation time and oligonucleotide concentration; however, all resulting DNA slides were suitable for biocatalytic lithography as described here.

Acknowledgment. The support of the NSF (CMMI-0609265) and NIH (GM61596) is gratefully acknowledged. B.N.V. acknowledges support of the Duke NSF IGERT award (DGE-0221632). Plasmid-containing hexahistidine-tagged exonuclease I was the generous gift of Prof. Brian Matthews, University of Oregon. Finally, we gratefully acknowledge the technical assistance of Alexander Shestopalov and Yi Yang.

Supporting Information Available: Additional experimental methods and results for biocatalytic-μCP, synthetic procedures, and characterization data of new compounds. This material is available free of charge via the Internet at http://pubs.acs.org.

JO0711541